C. R. Mecanique 339 (2011) 219–225

Contents lists available at ScienceDirect

Comptes Rendus Mecanique

www.sciencedirect.com

Experimental evidences of transition from mode I cracking to dilatancy banding

Mise en évidence expérimentale d'une transition entre fissuration en mode I et formation de bandes de dilatation

Alexandre I. Chemenda [a,*], Si-Hung Nguyen [a], Jean-Pierre Petit [b], Julien Ambre [a]

[a] *Géoazur, Université de Nice-Sophia Antipolis, CNRS, 250, rue Albert-Einstein, 06560 Valbonne, France*
[b] *Géosciences Montpellier, Université Montpellier 2, place E. Bataillon, 34095 Montpellier cedex 5, France*

ARTICLE INFO

Article history:
Received 5 November 2010
Accepted after revision 20 January 2011

Keywords:
Rupture
Rock mechanics
Fractures
Extension tests
Granular material
Dilation bands
Stability and bifurcation
Joints

Mots-clés :
Rupture
Mécanique des roches
Fractures
Essais en extension
Matériaux granulaires
Bandes de dilatance
Stabilité et bifurcation
Diaclases

ABSTRACT

Extension fractures of two types defined by the mean stress σ were generated in a synthetic rock analogue material. When σ is very small, the fractures are mode I cracks with smooth surfaces. At higher σ, these surfaces have plumose topography, with the amplitude increasing with σ. Both SEM observations and mechanical measurements show that fractures/discontinuities in the latter case are initiated as dilatancy localization bands. They form under tensile or slightly compressive normal stress and can be seen as running constitutive instabilities. The similarity between the plumose fractography of the experimental fractures and natural joints suggests similarity in the formation mechanism.

RÉSUMÉ

Deux types de fractures en extension dépendants de la contrainte moyenne σ ont été obtenus dans un matériau analogue de roches synthétique. Quand σ est très petit, des fractures en mode I se forment et présentent des surfaces lisses. A plus forte σ, des reliefs en structures plumeuses apparaissent sur les surfaces, dont l'amplitude s'accroit avec σ. Des observations au MEB et des mesures mécaniques montrent que dans ce dernier cas, ces fractures/discontinuités sont initiées en tant que bandes de localisation dilatantes. Elles se forment sous de faibles contraintes normales en traction ou en compression et sont interprétées comme des instabilités constitutives propageantes. La similarité entre la fractographie plumeuse expérimentale et celle des diaclases suggère la similarité des mécanismes de formation.

1. Introduction

Extension fractures orthogonal to the least principal stress σ_3 (the rock mechanics convention for the principal stresses is adopted here: $\sigma_1 > \sigma_2 > \sigma_3$, the compressive stress is positive) are of major importance in both engineering and natural/geological structures. The mechanism of their formation (or more exactly, of propagation from a preexisting flaw) is

* Corresponding author.
E-mail address: chem@geoazur.unice.fr (A.I. Chemenda).

1631-0721/$ – see front matter
doi:10.1016/j.crme.2011.01.002

generally considered to be related to the concentration of the tensile stress at the fracture tip zones that occurs due to the opening of the fracture walls under the remote load. This corresponds to the mode I or opening mode fracture. In spite of the apparent simplicity and wide use of this mechanism in both engineering and geological sciences, there are many problems/uncertainties with its practical applications (e.g., [1,2]), related notably to the inelastic behavior in the fracture tip zone, whose size in many cases remains undefined and can be very large [3]. The relative contribution of the brittle and plastic deformation in the fracture formation therefore remains uncertain.

The other approach to the fracture is the formation of deformation localization bands as constitutive instabilities resulting from elastic–plastic deformation bifurcation [4,5]. The localization bands can have different orientations including the orthogonal to σ_3 one [6–9], in which case they are called splitting or dilation bands. It is believed that such bands can result in the formation of extension fractures, but they (bands) were neither obtained/detected in the laboratory experiments, nor clearly observed in nature. In this paper we report the results of axisymmetric extension tests on a synthetic granular, frictional, cohesive and dilatant physical rock analogue material GRAM1, where such bands were obtained (a detailed description of GRAM1 and its physical analogy with rocks is presented in [10]). The accent is placed on the fractography and microstructure of the extension fractures generated under different confining pressure P. The fractography (and hence microstructure) was proved to be very sensitive to P, attesting to the change of the fracture mechanism with P: it goes from mode I to a running constitutive instability that results in the formation of dilatancy bands and, with further extension, in the opening fractures.

2. Experimental details

2.1. The rock analogue material GRAM1

The GRAM1 (Granular Rock Analogue Material 1) material is made of a finely ground powder of TiO_2 (average grain size is of ~ 0.3 μm) subjected to a hydrostatic pressure of $P^{fabr} = 2$ MPa at which the grains are bonded one to another by molecular and atomic forces (see [10] for details). Both axisymmetric compression and extension tests at different confining pressure P have shown that GRAM1 has cohesive, frictional, and dilatant properties very close to those of hard rocks [10]. Similar to rocks, GRAM1 samples exhibit macroscopic failure modes ranging from very brittle splitting to shear fracturing and compaction bands with P increase. However GRAM1 is less strong and rigid than rocks of about 2 orders of magnitude. The GRAM1 properties are physically similar to those of real rocks and can be up-scaled to rocks using the scaling factors [10]. The elastic moduli are $E = 6.65 \times 10^8$ Pa (Young's modulus), $\nu = 0.25$ (Poisson's ratio). The internal friction coefficient is $\alpha \approx 0.6$, and the dilatancy factor β (for extension conditions) varies from 0.4 at $P = 0.4$ MPa to -0.2 at $P = 1.3$ MPa (the latter corresponds to the brittle ductile transition). The density is 1723 kg/m^3, and the porosity is about 57%.

2.2. Procedure

We summarize here the main points of the detailed description in [10]. The tested GRAM1 samples were first loaded hydrostatically to a pressure P. Then they were unloaded at $P = \text{const}$ in the axial direction. At a certain deformation stage after the failure onset or just at the onset (which was detected by the stress jump on the stress–strain curves), the unloading was stopped. In order to investigate a possible influence of the unloading conditions on fractography and microstructure the samples were unloaded following two different paths. In the first path, the fractured sample was reloaded vertically to the initial hydrostatic state before a hydrostatic unloading to $P = 0$. The second path was applied when the final (peak) axial stress $\sigma_{ax}^{pk} = \sigma_3^{pk}$ was either tensile or slightly compressive. In the latter case, σ_{ax}^{pk} was kept constant and P was reduced to the value of this stress. The complete unloading was hydrostatic. In the case where σ_{ax}^{pk} was tensile, it was increased to a slightly compressive value maintained constant during P reduction up to this value. Then the complete unloading was done hydrostatically. Cylindrical samples were used when failure occurred at a compressive axial stress, whereas dog–bone samples were used in the tests where the tensile axial stress was required, i.e., in low-P tests [10].

3. Fracturing types and fractography

As in rocks, the orientation of fractures generated in the GRAM1 samples depends on the confining pressure P (or the mean stress σ). At $P > 0.7$ MPa ($\sigma > 0.48$ MPa), the angle ψ between σ_1 and fractures grows with P (Domain III in Fig. 1). At $P < 0.7$ MPa, ψ is close to zero (Domains I and II in Fig. 1), i.e. the fractures are perpendicular to $\sigma_{ax} = \sigma_3$. Below we focus on these σ_3-perpendicular fractures that form dynamically, which is attested by acoustic emissions (sharp snapping noises) as well as by the stress jumps in the stress–strain curves after reaching σ_{ax}^{pk} [10].

The fractures represent very thin (hardly visible) discontinuities at the sample surface (Fig. 2(a)). The fracture surfaces displayed after the opening of a discontinuity, exhibit faint and delicate plumose topography consisting in ridges and troughs forming a diverging pattern. At relatively high pressures, the pattern is complicated with steps (Fig. 2(d)). With P reduction, this small-scale topography becomes less expressed. At $P <\sim 0.2$ MPa ($\sigma < 0.11$ MPa), it disappears completely (Fig. 2(b)).

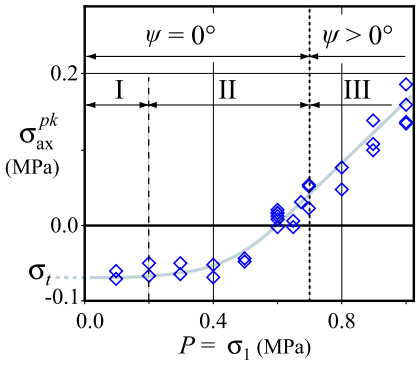

Fig. 1. Axial peak stress $\sigma_{ax}^{pk} = \sigma_3^{pk}$ *vs* confining pressure P in GRAM1 extension tests. ψ is the angle between the fractures/discontinuities and the maximal compressive stress σ_1. I, II and III are the domains of Mode I fracturing, dilatancy banding, and shear banding, respectively.

Fig. 1. Valeurs pic des contraintes axiales $\sigma_{ax}^{pk} = \sigma_3^{pk}$ en fonction de la contrainte moyenne σ et de la pression de confinement P ($P = \sigma_1$). ψ est l'angle entre les fractures/discontinuités et σ_1. Dans l'interprétation proposée, I, II et III sont respectivement les domaines de la fracturation en Mode I, de la formation des bandes de dilatance, et des bandes de cisaillement.

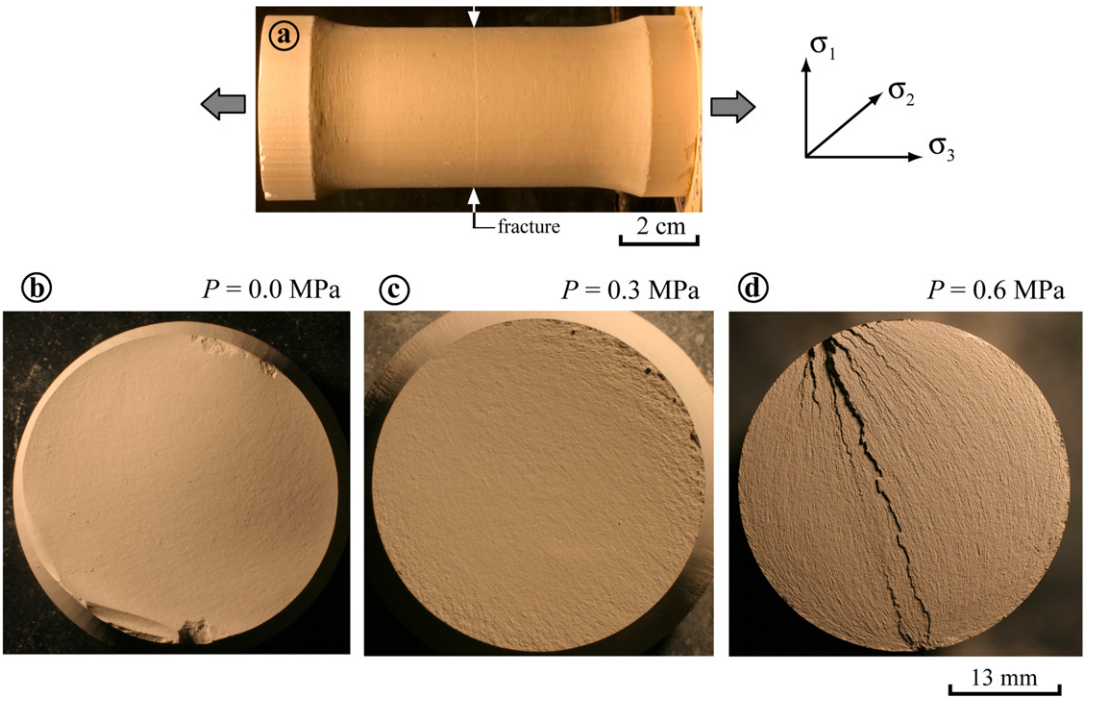

Fig. 2. GRAM1 samples fractured in extension tests. (a) General view of a dog–bone sample. (b) to (d) Surfaces of the σ_3-orthogonal fractures generated in GRAM1 at different confining pressure P.

Fig. 2. Eprouvettes de GRAM1 fracturées lors d'essais en extension. (a) Vue générale d'un échantillon «dog bone» fracturé au milieu. (b) à (d) Surfaces de fractures orthogonales à σ_3 générées à différentes pression de confinement P.

The value of σ_{ax}^{pk} at σ_3-orthogonal fracturing reduces with P reduction from slightly positive values at $0.6 < P < 0.7$ MPa to growing negative values at $P < 0.6$ MPa, reaching practically a plateau of $\sigma_{ax}^{pk} = -\sigma_t$ at $P < 0.3$ MPa, Fig. 1 ($\sigma_t = 0.07$ MPa is the GRAM1 tensile strength).

4. Microstructural data and analysis

The σ_3-perpendicular discontinuities were thus shown to form at compressive or tensile (negative) σ_3 much higher than $-\sigma_t$ (Fig. 1). At formation these discontinuities are not opened. They can easily be opened if axial extension of the sample continues after fracturing. To analyze the pre-opening structure of these discontinuities, tests were conducted where extension was stopped just after reaching σ_{ax}^{pk}. Then the sample was unloaded following one or the other unloading path de-

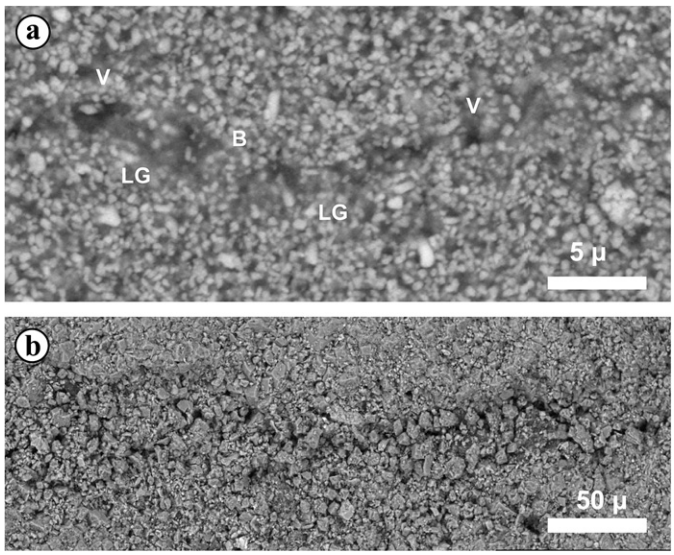

Fig. 3. Aspects of experimental (a) and natural (b) dilatancy bands. (a) SEM photomozaics (backscattered electron micrographies) of the band in GRAM1 sample fractured at $P = 0.6$ MPa. The band area was impregnated with a low-viscosity epoxy resin which penetrated the pores both inside and outside the band. After the polymerization (solidification) of the resin, the sample was cut perpendicularly to the band and the section was carefully polished before observation. The band represents an alignment of voids (V), loose grain zones (LG) where the decompacted grains are surrounded by the resin (blurred grey background around the grains), and by zones (bridges (B)) of apparently intact material. (b) SEM image of a fine discontinuity (incipient joint) parallel to a dense joint set in dolomicrites (see details in Fig. 4). It shows a band with loose/dislocated dolomite grains and increased porosity (compared to the host rock). In both SEM images, the thickness of the band is several grain diameters.

Fig. 3. Aspects des bandes de dilatance expérimentales (a) et naturelles (b). (a) Photomosaïque au microscope électronique à balayage (électrons rétrodiffusés) d'une bande dans une éprouvette de GRAM1 fracturée à $P = 0.6$ MPa. Le matériau a été imprégné avec une résine époxy de basse viscosité qui a pénétré dans et autour de la bande. Après polymérisation (solidification) de la résine, l'éprouvette a été sciée perpendiculairement à la bande, et la section polie avec soin avant l'observation. Les structures sont caractéristiques et ne peuvent être introduites par le sciage ou le polissage. A l'échelle présentée, la bande apparaît formée par un alignement de vides (V), de zones de grains lâches (LG) où les grains décompactés apparaissent inclus dans la résine (zones grisâtres troubles autour des grains), et par des ponts (B) de matériel apparemment intact. (b) Image au microscope électronique à balayage (électrons rétrodiffusés) d'une fine discontinuité (diaclase embryonnaire) parallèle à une famille de diaclases denses dans une dolomicrite (voir contexte dans la Fig. 4). L'image montre une bande constituée de grains de dolomie disloqués/décompactés avec accroissement de la porosité (par rapport au reste du matériau). Sur les 2 images MEB, l'épaisseur de la bande est de plusieurs diamètres de grains.

scribed above. After consolidation by a resin (see caption of Fig. 3 for details), the discontinuities were observed in Scanning Electron Microscope (SEM) and were shown to represent sinuous bands of heterogeneously damaged material (Fig. 3(a)). The bands consist of zones of loose grains, voids of different shapes and sizes, as well as bridges of apparently intact material. There is neither along-band progressive or monotonous evolution of the aspect of damage, nor a progressive separation/aperture of the walls of the band (future fracture). The walls are not separated at all. The band material underwent damage and decompaction resulting in the porosity increase, corresponding to the dilatancy. Reynolds [11] defined it as an inelastic volume/porosity increase of the material during its deformation. In the following discussion the term dilatancy (and dilatant) is used in Reynolds' sense as referring to a deformation and not to a displacement (as a fracture opening, for example). Thus the deformation bands obtained in our experiments are dilatancy bands. The SEM images do not allow description of the grain scale mechanism of deformation within the bands, although the grain separation is obvious. Due to the non-planar geometry of the bands, grain sliding (micro-shearing) accompanied by translation and rotation are obviously also present. All these complex movements distributed in 3D result in the porosity increase within the band.

Figs. 2 and 3(a) present the results of the tests where GRAM1 samples were unloaded after fracturing following the first path. The fractographic pattern and dilatancy band microstructure are practically the same for the second path. The non-dependence of the failure structure on the loading path was not obvious beforehand and is explained as follows. The fracturing occurs when the deviatoric stress reaches the maximum value. For both unloading paths the deviatoric stress reduces (since the stress state approaches the hydrostatic equilibrium): the stress state shifts from the yield/failure surface (where it was at the moment of rupture) inside this surface (toward the hydrostatic axis) where only elastic response is possible. Therefore the band structure acquired at the moment of its formation is not modified during the post formation unloading for either path.

5. Mechanisms of formation

The data presented suggest that extension fractures include fractures of two types corresponding to different mechanisms of formation.

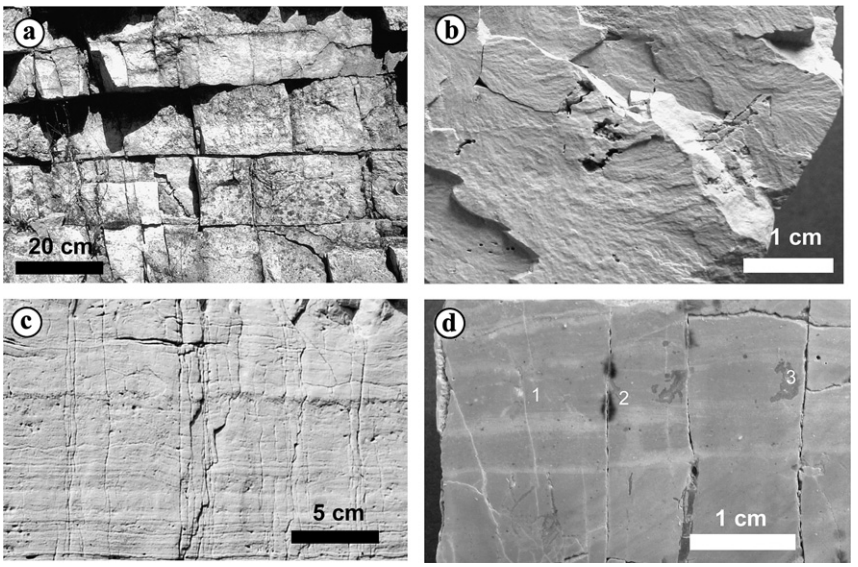

Fig. 4. Macroscopic aspects of dilatancy joints in Hettangian dolomicrites of the Larzac Plateau border (South of France). (a) The "cubic dolomite" affected by orthogonal joint sets in tabular layers. (b) Plumose features on an open joint limiting the dolomicrite sample from which the SEM image of Fig. 3(b) was obtained. (c) Aspect of vertical traces of unopened dilatancy band/incipient joint on a natural surface in dolomicrite. Traces are etched by weathering. The horizontal laminations correspond to stromatolitic deposits. (d) Sawcut and polished section of a sample of dolomicrite (the same as in (c)) evidencing more traces than on the natural (not treated) surfaces of the sample. 1, Trace of an unopened embryonic joint (dilatancy band) similar to that from which the SEM image of Fig. 3(b) was obtained; 2, Trace of a small joint with a small shear offset; 3, Trace of a partly open joint.

Fig. 4. Aspects macroscopiques des joints de dilatance dans les dolomicrites hettangiennes de la bordure du plateau du Larzac (Sud de la France). (a) aspect de la « dolomie cubique » résultant de la présence d'un réseau de diaclases orthogonales dans les couches tabulaires. (b) Structures plumeuses sur un joint ouvert limitant l'échantillon dont est extraite l'image MEB de la Fig. 3(b). (c) Aspect sur une surface naturelle des traces verticales petites bandes de dilatance/diaclases non ouvertes dans les dolomicrites. Ces traces sont soulignées par l'altération superficielle. Les laminations horizontales resultent de dépôts stromatolitiques. (d) Section polie d'un échantillon de dolomicrite (le même qu'en (c)) montrant des traces plus denses que sur les surfaces naturelles de l'échantillon. 1 est la trace d'une diaclase embryonnaire non ouverte (bande de dilatance) similaire à celle examinée au MEB dans la Fig. 3(b) ; 2 est la trace d'une petite diaclase avec un léger décalage cisaillant ; en 3 la diaclase est partiellement ouverte.

Fractures with smooth-surface forming at very low σ at tensile σ_3 reaching the material tensile strength σ_t are Mode I (or opening mode) cracks.

Fractures/discontinuities with plumose-surface are not simple (zero-thickness) cracks but represent narrow bands of damaged material with reduced cohesion and increased porosity/volume. They are therefore the dilatancy bands representing zones of weakness. The bands are initially closed. They become fractures only after their *post mortem* opening. No direct trace of the band existence remains after its opening. The indirect expression of the band is the plumose relief of its boundaries, forming the fracture walls after the band opening. The plumose fractography is thus defined by the decohesion pattern of the material within the band and represents a diverging delicate network of ridges and grooves stemming from an initiation point. This pattern, very typical of the fractography of geological joints, is commonly interpreted as resulting from a propagating rupture/fracture [12]. That would suggest that the band is a propagating feature, and also point to a Mode I (opening mode) type crack mechanism. This is however impossible as the band was not opened before its *post mortem* separation. The likely mechanism is a constitutive instability initiated as a deformation bifurcation and then evolving into the post-bifurcation stage toward large inelastic deformation. This deformation can be simulated in dynamic numerical models [13–15]. They confirm the predictions of the bifurcation theory dealing with the conditions of the bifurcation onset, the orientation and the average spacing of the bands. But they also show that even at the onset in the homogeneous stress–strain field, the deformation bands are not continuous structures. They can propagate with increasing deformation [15]. The full understanding of the mechanism cannot be reached without combined experimental, theoretical, and numerical investigations.

6. Application to natural fractures

The experimental fractures/discontinuities formed as dilatancy bands are very similar to geological joints. Not only the orientation of experimental and geological joints is orthogonal to σ_3, but also they exhibit the same striking plumose fractography with diverging delicate network of ridges and grooves (Figs. 2(d), 4(b) and 5). This suggests that the natural joints with plumose fractography were initially dilatancy bands. This interpretation is opposite to that commonly used in geological literature where joints are considered to form as Mode I fractures (e.g., [17–19]). Therefore, the research of dilatancy band structure in non-open yet natural joints is of major interest. The absence of such observations in literature can be

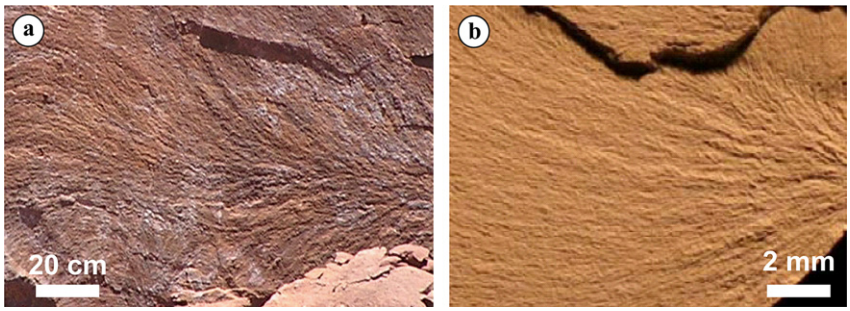

Fig. 5. (a) Natural plumose on a joint of an N110 joint sets in the pelites of the Permian Lodève basin, South France (geological details are in [16]). (b) Plumose generated in GRAM1 extension test at $P = 0.6$ MPa.

Fig. 5. (a) Figure plumeuse naturelle sur une diaclase d'une famille N110 appartenant au réseau de fractures du bassin Permien de Lodève, sud de la France [16]. (b) Figure plumeuse générée dans GRAM1 lors d'un essai en extension à $P = 0.6$ MPa.

explained by the very common aperture of joints in outcropping conditions and by the transformation of the internal structure by diagenetic/epigenetic processes, in particular dissolution and recrystallization. Fig. 3(b) shows the first micrograph of a natural untransformed incipient joint. It has been obtained on a small joint-parallel discontinuity belonging to densely jointed Jurassic dolomicrites (fine grained carbonate rock) of Languedoc (the so-called "cubic dolomite", Fig. 4(a)) where the opened joints exhibit fine plumose features, Fig. 4(b). The material decohesion with porosity increase in Fig. 3(b) are similar to those in the band in GRAM1 (Fig. 3(a)). There is also some similarity with the non-cataclastic (disaggregation) band images of [20] from the Nubian Sandstone of Sinaï, and with the hitherto unique image of a dilation/dilatancy band observed in poorly consolidated sands of California [21]. The dilatancy band structures could be quite current in nature. Their evidence, however, requires the observation of embryonic (still closed) structures (Fig. 4(d), 1), which are not necessarily visible by naked eye. As mentioned, fracture diagenesis may destroy the initial structure of the band, which is very likely in most of carbonates.

The presented observations reinforce the conclusion that the formation mechanism of plumose-bearing natural joints can be similar to that in GRAM1, i.e., is a running dilatancy banding. The mechanism suggests the name of this type of joints: dilatancy joints. The term "Mode I joints" could apply to joints forming through Mode I cracking attested by smooth fracture surfaces.

A major application of the proposed new jointing mechanisms concerns joint spacing prediction which is essential in defining the reservoir properties and therefore is a fundamental parameter for reservoir modeling. In Mode I conditions, the spacing λ between joints cannot be smaller than a certain value comparable to the layer thickness. This conclusion follows from the concept of fracture saturation according to which the stress shadow effect around already formed joints impedes the formation of a nearby joint [22,23]. This is not the case for localization bands, where λ is defined by the stress state type, and by all constitutive parameters, particularly the hardening modulus. The spacing can vary from infinity to the thickness of the band independently from the layer thickness [13,14]. In field conditions, joint sets with tight spacing (not "allowed" by the fracture saturation concept) are frequent.

Acknowledgements

This work has been done within the framework of the Geo-FracNet consortium sponsored by SHELL and TOTAL who are gratefully acknowledged. We also thank the reviewers for the useful suggestions.

References

[1] J.G.M. Van Mier, Fracture Processes of Concrete: Assessment of Material Parameters for Fracture Models, CRC Press, Boca Raton, FL, USA, 1997, p. 448.
[2] Z.P. Bažant, J. Planas, Fracture and Size Effect in Concrete and Other Quasibrittle Materials, CRC Press, Boca Raton, FL/London, 1998.
[3] S. Mindess, Fracture process zone detection, in: S.P. Shah, A. Carpinteri (Eds.), Fracture Mechanics Test Methods for Concrete, E&FN Spon, London/New York, 1991, pp. 231–261.
[4] J.W. Rudnicki, J.R. Rice, Conditions for the localization of deformation in pressure-sensitive dilatant materials, J. Mech. Phys. Solids 23 (6) (1975) 371–394.
[5] J.R. Rice, The localization of plastic deformation, in: W.T. Koiter (Ed.), Theoretical and Applied Mechanics, I.C.T.A.M., vol. 1, North-Holland Pub. Co., 1976, pp. 207–220.
[6] D. Bigoni, T. Hueckel, Uniqueness and localization–I. Associative and non-associative elastoplasticity, Int. J. Solids Struct. 2B (2) (1991) 197–213.
[7] N.S. Ottosen, K. Runesson, Properties of discontinuous bifurcation solutions in elasto-plasticity, Int. J. Solids Struct. 27 (1991) 401–421.
[8] G. Perrin, J.B. Leblond, Rudnicki and Rice's analysis of strain localization revisited, J. Appl. Mech. 60 (1993) 842–846.
[9] K.A. Issen, J.W. Rudnicki, Conditions for compaction bands in porous rocks, J. Geophys. Res. 105 (2000) 21529–21536.
[10] S.-H. Nguyen, A.I. Chemenda, J. Ambre, Influence of the loading conditions on the mechanical response of granular materials as constrained from experimental tests on synthetic rock analogue material, Int. J. Rock Mech. Min. Sci. 48 (2011) 103–115, doi:10.1016/j.ijrmms.2010.09.010.
[11] O. Reynolds, On the dilatancy of media composed of rigid particles in contact, with experimental illustrations, Phil. Mag. 20 (5) (1885) 469–481.
[12] D. Bahat, Tectono-Fractography, Springer-Verlag, 1991.

[13] A.I. Chemenda, The formation of shear-band/fracture networks from a constitutive instability: Theory and numerical experiment, J. Geophys. Res. 112 (2007) B11404, doi:10.1029/2007JB005026.
[14] A.I. Chemenda, The formation of tabular compaction-band arrays: Theoretical and numerical analysis, J. Mech. Phys. Solids 57 (2009) 851–868.
[15] A.I. Chemenda, Origin of compaction bands: Anti-cracking or constitutive instability?, Tectonophys. 499 (2011) 156–164, doi:10.1016/j.tecto.2011.01.005.
[16] G. de Joussineau, L. Bazalgette, J.-P. Petit, M. Lopez, Morphology, intersections, and syn/late-diagenetic origin of vein networks in pelites of the Lodève Permian Basin, Southern France, J. Struct. Geol. 27 (2005) 67–87.
[17] D. Bahat, Theoretical considerations on mechanical parameters of joint surfaces based on studies on ceramics, Geol. Msg. 116 (1979) 81–92.
[18] D.D. Pollard, A. Aydin, Progress in understanding jointing over the past century, Bull. Geol. Soc. Am. 100 (1988) 1181–1204.
[19] G. Mandl, Rock Joints. The Mechanical Genesis, Springer, 2005.
[20] H.R. Fossen, A. Schultz, Z.K. Shipton, K. Mair, Deformation bands in sandstone: A review, J. Geol. Soc. London 164 (4) (2007) 755–769, doi:10.1144/0016-76492006–036.
[21] X. Du Bernard, P. Eichhubl, A. Aydin, Dilation bands: A new form of localized failure in granular media, Geophys. Res. Lett. 29 (24) (2002) 2176–2180, doi:10.1029/2002GL015966.
[22] T. Rives, M. Razack, J.-P. Petit, K.D. Rawnsley, Joint spacing periodicity: Field data, analog and numerical modelling, J. Struct. Geol. 14 (8–9) (1992) 925–937.
[23] T. Bai, D.D. Pollard, Fracture spacing in layered rocks: A new explanation based on the stress transition, J. Struct. Geol. 22 (2000) 43–57.